

Diffusion between evolving interfaces

Janne Juntunen* and Juha Merikoski†
Department of Physics, University of Jyväskylä
 (Dated: 24 September 2010)

Diffusion in an evolving environment is studied by continuous-time Monte Carlo simulations. Diffusion is modelled by continuous-time random walkers on a lattice, in a dynamic environment provided by bubbles between two one-dimensional interfaces driven symmetrically towards each other. For one-dimensional random walkers constrained by the interfaces, the bubble size distribution dominates diffusion. For two-dimensional random walkers, it is also controlled by the topography and dynamics of the interfaces. The results of the one-dimensional case are recovered in the limit where the interfaces are strongly driven. Even with simple hard-core repulsion between the interfaces and the particles, diffusion is found to depend strongly on the details of the dynamical rules of particles close to the interfaces. *Article reference: Journal of Physics: Condensed Matter 22, 465402 (2010).*

PACS numbers: 87.16.dp, 05.40.-a, 02.50.Cd, 66.10.cg, 64.60.De

I. INTRODUCTION

Diffusion phenomena are ubiquitous in nature, familiar examples ranging from heat conduction to osmosis. Often diffusion occurs in a random or nonideal environment as it does, for example, in the presence of mobile or immobile (in the time scale of diffusion) lattice imperfections. Due to the complexity of real materials, transport has been considered within simplified theoretical frameworks, often utilizing the random-walk picture to describe some assumed underlying microscopy. Novel biophysical applications can be expected to emerge for transport restricted by soft (and fluctuating) interfaces forming narrow or even nanoscale channels [1]. In particular the crossover from bulk-dominated to boundary-dominated diffusion is of considerable theoretical and experimental interest.

The study of random walks in a random environment (RWRE) has a long history and since the results [2, 3] from the 70's, as reviewed in Ref. [4], a vast amount of information has been accumulated. This randomness has been considered to manifest itself as non-homogeneous transition rates [5–7]. Spatially, (frozen) transition rates can sometimes be described by random walkers like in the Sinai model [8]. In general, theoretical studies have mostly been limited to models, where the environment, including the possible geometric constraints, is either stationary or fast compared with the jump rate of the walkers. The mathematical problem of the random walk in an uncorrelated fluctuating environment has been considered in Ref. [9]. The asymptotics of diffusion in continuum under a random forcing in the presence of damping were analyzed in Ref. [10] and diffusion in restricted geometries with homogeneous transition rates was considered in Ref. [11]. Two-species zero-range process [12, 13] with suitably chosen transition rates leads to dynamics which can be considered as a diffusing particle in an

evolving environment [14]. However, in existing studies the focus has not been in (undriven) diffusion. In Ref. [15] Sané *et al.* considered a situation, where particles are immersed in a background fluid inside a narrow channel. From the point of view of a single particle in the dilute limit, this could be interpreted as diffusion in a dynamic environment. In that work the focus was on the transition from single file dynamics to Fickian diffusion. The existing studies on particle dynamics in the presence of interfaces are mainly for particles immersed in a driven liquid [16]. A related problem, the influence of geometry fluctuations on lateral diffusion in biological systems was studied very recently in Ref. [17], where it is noted that geometry fluctuations at a finite scale can affect diffusion at all scales.

In this Article, we consider diffusion in a dynamic restricting environment, inside open evolving 'bubbles' between two interfaces. For this, we combine two most simple models, the solid-on-solid (SOS) model of interfaces and the continuous-time random walk on a lattice, models that are widely used and known to describe well interface fluctuations and particle diffusion. To be more specific, we study diffusion on a lattice in the environment produced by the dynamics of the BCSOS2-model introduced in Ref. [18], containing two non-intersecting interfaces driven against each other. Thus, due to the interface dynamics, the actual transition rates of a diffusing particle become dependent on time and position, when the jumps of the particle are possible only inside the 'bubbles' between the interfaces. Diffusion in the hydrodynamic limit will then depend on the dynamics of the bubbles, e.g. through their growth and merging. We shall concentrate on cases, where the particles do not affect the motion of the interfaces so that the dynamics of the two interfaces, e.g. the bubble-size distributions and their correlations, are in principle known [18] and thus, in addition to simulations, analytical arguments can be developed for various limits, which is the particular strength of the model. We use our model as a testing ground for various ideas describing different regimes of behavior of the diffusion coefficient. In addition, we study the possible

*Electronic address: janne.k.juntunen@jyu.fi

†Electronic address: juha.t.merikoski@jyu.fi

consequences of various choices of microscopic dynamics on the interaction of the interfaces and the diffusing particle. To reduce the dimension of the parameter space, the models we combine are relatively simple. However, most of our results are expected not to be dependent on the details of the model, but are characteristic of systems, where the size distribution of the bubbles and their dynamics (at the bubble scale) inside a material or at an interface between two materials become the rate-limiting factor for diffusion (at the hydrodynamic scale).

This paper is organized as follows. In Sec. II we define the evolving environment provided by the two interfaces and the dynamic rules of the walker (particle) in detail. After that, in Sec. III, we describe the algorithms needed for efficient simulation of the combined dynamics and the sampling of the main quantities. An experimentally oriented reader could first skip Secs. II-III and proceed to Sec. III D, where we briefly describe the parameters and their physical interpretation. Our results for the combined interface and particle dynamics are presented in Secs. IV-V. A concluding discussion of our results is given in Sec. VI.

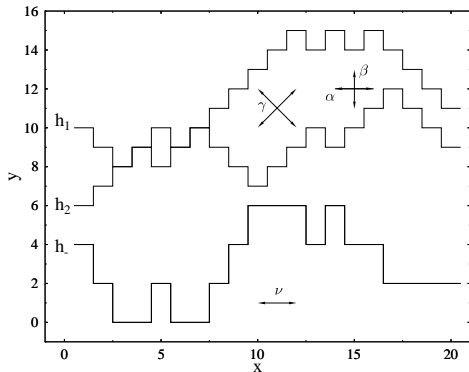


FIG. 1: A snapshot of the two interfaces h_1 and h_2 and the possible jumps of a diffusing particle with their attempt rates α , β , γ and ν . Also the corresponding difference $h_- = h_1 - h_2$ is shown. The jumps of the particle are possible only within the bubbles (open spaces) between the interface. The jump rate ν is for the one-dimensional motion (see dynamics 4 in text) depending only on h_- . To simplify the discussion, when possible, in the text the various rate parameters are collectively referred to simply as μ in such a way that the total rate for the particle to attempt a jump is μ .

II. MODELS

A. Model for the interface dynamics

The evolving environment for diffusion is produced by the dynamics of the BCSOS2 model that we introduced and discussed in Ref. [18]. Below we give only a brief description of the BCSOS2 model so that the dynamical rules for diffusion become well defined for the present study. The BCSOS2 model is constructed by letting two one-dimensional BCSOS interfaces [20] interact with each others.

The location or the 'height' of a single BCSOS interface is described by a function $h_i(x, t)$ such that, for every site $x = 1, \dots, L$,

$$h_i(x+1, t) - h_i(x, t) = \pm 1, \quad (1)$$

where we without loss of generality assume that the possible values of h_i are integers. With this restriction on local configurations of the interfaces, only two kinds of processes, adsorption (h_i locally increases) and desorption (h_i locally decreases), are available. In our continuous-time model (see Sec. III), the parameters p_i and q_i give the transition rates of adsorption and desorption events, respectively, for transitions allowed by the condition (1). In what follows, time and various rates are measured in units where $p_i + q_i = 1$.

In the BCSOS2 model there are two interfaces, $h_1(x, t)$ and $h_2(x, t)$, such that $h_i(x, t)$ is an even (odd) integer for odd (even) values of x , see Fig. 1. The coupling between the interfaces is produced by demanding that they cannot intersect:

$$h_1(x, t) \geq h_2(x, t) \quad \text{for all } x, t. \quad (2)$$

We also impose the periodic boundary conditions $h_i(x, t) \equiv h_i(x + L, t)$ for $i = 1, 2$. In the full BCSOS2 model, there are then four parameters $[(p_1, q_1), (p_2, q_2)]$ defining the transition rates for the interfaces h_1 and h_2 , respectively. To further limit the parameter space, we shall restrict the discussion to the symmetric case $p_1 = q_2$ and $q_1 = p_2$ (see Ref. [18]) so that the behavior of the BCSOS2 system is defined by one parameter, the driving parameter f defined as

$$f \equiv p_2/q_2 - 1. \quad (3)$$

For large f the interfaces are strongly driven against each other and for $f \rightarrow 0$ they become free. We also define the sum and difference processes defined via $h_{\pm} = h_1 \pm h_2$, where the sum process h_+ describes the wandering of the interfaces together and the difference process h_- is positive inside the bubbles and zero elsewhere [18]. The non-crossing condition of Eq. (2) is equivalent to $h_-(x, t) \geq 0$. The interfaces h_{\pm} are then of the RSOS type [20], obeying $h_{\pm}(x+1, t) - h_{\pm}(x, t) = -2, 0, +2$. An example of h_1 and h_2 and the corresponding h_- configuration is shown in Fig. 1.

B. Models for particle diffusion

We consider a single point-sized particle diffusing between the interfaces $h_1(x, t)$ and $h_2(x, t)$ on a lattice (x, y) . The lattice point coordinates in the horizontal direction are the same $x = 1, \dots, L$ as for the interface model above, again with periodic boundary conditions, c.f. Fig. 1. In the 'vertical' direction, the lattice is infinite and the coordinates are integers $y = \dots, -2, 1, 0, 1, 2, \dots$ and thus coincide with the possible values of h_1 and h_2 .

We shall denote the location of the particle by (x_p, y_p) . The particle does not affect the dynamics of the interfaces but, if needed, a moving interface can push the particle the distance of one or two lattice units in the vertical direction such that the location of the particle also after the change of the interface configuration satisfies the condition

$$h_2(x_p, t) \leq y_p \leq h_1(x_p, t). \quad (4)$$

These are moves of the particle forced by the interface motion.

For diffusive moves of the particle, the following two rules are imposed in all cases: First, for a jump $(x_p, y_p) \rightarrow (x'_p, y'_p)$ to be possible, the product of the interface height differences on the departure site and the arrival site is non-zero: $h_-(x_p, t)h_-(x'_p, t) > 0$ *i.e.* the channel for the jump between the interfaces must be open at both ends of the jump. Second, an attempted jump arriving outside the region bounded by the interfaces is blocked. In the actual dynamics, the direction of an attempted jump is chosen without any prior knowledge of the ability of the particle to perform the jump.

For diffusion on the square lattice there are a few natural choices for the possible particle jumps $(x_p, y_p) \rightarrow (x'_p, y'_p)$

Dynamics $m = 1$: The most obvious case are the nearest-neighbor jumps such that the particle jumps in the horizontal direction $(x_p, y_p) \rightarrow (x_p \pm 1, y_p)$ with the attempt rate α and in the vertical direction $(x_p, y_p) \rightarrow (x_p, y_p \pm 1)$ with the attempt rate β . We set $\alpha = \beta$ so that the total attempt rate of the particle is $\mu = 4\alpha$.

Dynamics $m = 2$: The particle jumps diagonally, *i.e.* $(x_p, y_p) \rightarrow (x_p \pm 1, y_p \pm 1)$ independently, with the attempt rate γ . The total attempt rate is then $\mu = 4\gamma$. This process is expected to be efficient on tilted sections of the interfaces like the rightmost part of the snapshot configuration in Fig. 1.

Dynamics $m = 3$: This is a combination of the jumps available in dynamics 1 and 2. In this work we chose $\alpha = \beta = \gamma$ so that $\mu = 8\alpha$.

In addition to the three models above, which we shall call two-dimensional particle dynamics, we consider simplified dynamical rules, which will be called one-dimensional:

Dynamics $m = 4$: In this model only the x coordinate of the particle matters and the particle is allowed to perform the jump $(x_p, y_p) \rightarrow (x'_p, y'_p)$ whenever the channel is open, *i.e.* $h_-(x_p, t)h_-(x'_p, t) > 0$. Then the effect of

the interface dynamics on the possibility of the particular jump is fully determined by $h_-(x, t)$ and diffusion is most directly controlled by the bubbles. In this case, in addition to the jump of the particle in the horizontal direction, there is, when needed, a move in the vertical direction over one lattice unit to keep the particle between the interfaces such that $h_2(x_p, t) \leq y_p \leq h_1(x_p, t)$. The attempt rate of the jump in this case is denoted by ν . The effect of forced moves on waiting times of the particle in the continuous-time dynamics is discussed in more detail in Sec. III B.

III. NUMERICAL METHODS

A. Interface dynamics

For the dynamics of the interfaces, which is the most time-consuming part of the numerics, we used the so-called N -fold [21] algorithm in our continuous-time Monte Carlo simulations. In the N -fold algorithm the possible transitions are divided into N classes according to their probabilities. After finding those classes, one finds all lattice points x , which belong to a certain class j . The next step is to calculate the set of time-dependent variables $Q_i = \sum_{k=1}^{i \leq N} n_{j_k} P_{j_k}$, where n_{j_k} is the number of those lattice points which belong to the class j_k and P_{j_k} is the probability associated with j_k . The class j of the event, which will occur, is next determined by finding j such that $Q_{j-1} \leq R < Q_j$, where R is a random number with uniform distribution in the interval $(0, Q_N]$. After finding the class, one randomly chooses a location (on h_1 or h_2) from this class. The waiting time for something to happen in the system consisting of the two interfaces then is $\Delta t_I = -\ln(R_1)/Q_N$, where R_1 is a random number with uniform distribution in the interval $[0, 1)$.

B. Particle dynamics

To restrict the dimension of the parameter space, in our simulations we only consider cases where all possible attempts (see Fig. 1) of the particle to jump (within a given dynamics m) occur at the same rate as described in Sec. II B. For simplicity and when possible, we shall denote by μ the total jump rate of a free particle, which is then determined by the parameters α, β, γ and ν relevant in each case. In the presence of the interfaces this will become the total attempt rate such that with rate μ the particle will try to jump in a direction chosen randomly from the list of allowed processes. The waiting time Δt_P after which the particle tries to jump is drawn from the exponential distribution $\Delta t_P = -\ln(R_2)/\mu$, where R_2 is another uniformly distributed random number in the interval $(0, 1]$.

In the combined model containing both the interfaces and the particle, the particle does not affect the dynamics of the interfaces, which will evolve as described in the

first paragraph above. To include the diffusing particle, we need two waiting times: the waiting time Δt_I of the interface system and the waiting time Δt_P of the particle. We then keep track of two times: First, the latest instant of real time t_I , when there was a move in the interface system. Second, the latest instant of time t_P , when there was either an attempt of the particle to jump or a forced move of the particle. Then, if $t_I + \Delta t_I < t_P + \Delta t_P$, the next event in the system will be a move of the interface, otherwise the next event will be an attempt to move the particle.

After this, there still are in the continuous-time dynamics two obvious ways to handle the forced moves (in dynamics $m=1,2,3$): (A) The clock of the particle remains intact in a forced move or (B) its waiting time Δt_P for the particle is updated after it. We shall consider both choices since they produce quite different results and both can be physically justifiable from some microscopy. With this choice the dynamics of the combined model becomes defined.

C. Sampling of main quantities

The sampling of the observables was done with a constant time interval after reaching the steady state from an initial configuration consisting of two completely disordered interfaces at a fixed distance from each other. With the N -fold method reaching the steady state for interface configurations turns out not to be very difficult but especially for sampling of diffusion quite long runs were required.

Typically of the order of 10^3 independent runs were performed for the interfaces in such a way that there were 10^2 particles diffusing (independently of each other) between the interfaces, the linear size of the simulation cell being $L = 100$ (for the finite-size scaling studies mentioned in the text larger systems were used). The reason for this procedure is that the dynamics of the interfaces even with the N -fold algorithm is computationally the most time-consuming part of the simulation, so we used each sequence of interface configurations to produce many particle trajectories, the total statistics thus being of the order of 10^5 .

To characterize the statistical properties of the interfaces h_1 and h_2 , we use their roughness or width [20] defined as

$$W(f) = \sqrt{\langle |h_i(x, t) - \bar{h}_i(t)|^2 \rangle} \quad (5)$$

Here $i = 1, 2$ and $\bar{h}_i(t)$ is the spatially averaged height of the interface configuration at time t , and the angle brackets denote ensemble average, *i.e.* average over independent simulations. The kink density $\bar{k}(f)$ is the density of those locations x , for which $h_i(x-1, t) \neq h_i(x+1, t)$ for each of the interfaces $i = 1, 2$ separately. This definition follows from the fact that a BCSOS interface even in the flat state has an intrinsic roughness, because

$|h_i(x, t) - h_i(x \pm 1, t)| = 1$. In the notations for these quantities we suppress the dependence on system size L .

The bubble size distribution per site was sampled at the same instant of times as the width of the interfaces. It gives the probability that a randomly chosen location x belongs to a bubble of size ℓ , which is the length of the bubble in x direction. We shall be interested in bubble size distributions $P_j(\ell, f)$, normalized such that only bubbles with $j \leq \ell < L$ are taken into account, $\sum_{\ell=j}^{L-1} P_j(\ell, f) = 1$, so that they are related by

$$P_j(\ell, f) = P_0(\ell, f) \left[1 - \sum_{\ell=0}^{j-1} P_0(\ell, f) \right]^{-1}. \quad (6)$$

In this $\ell = 0$ means that $h_-(x, t) = 0$ for site x . In the configurations, where the interfaces did not touch each other at all, the bubble size was recorded as a count in bin $\ell = L$. For certain purposes we also sample the bubble size distributions normalized for $j \leq \ell \leq L$, which we denote by $P_j^*(\ell, f)$, so that $\sum_{\ell=j}^L P_j^*(\ell, f) = 1$. In addition, we compute the (physical) average bubble size $\bar{\ell}(f)$ and also $\bar{\ell}^*(f)$ defined as

$$\bar{\ell}(f) = \sum_{\ell=0}^{L-1} \ell P_0(\ell, f) \quad \bar{\ell}^*(f) = \sum_{\ell=0}^{L-1} \ell P_0^*(\ell, f). \quad (7)$$

The mean waiting time for the change of the bubble size we shall denote by $\bar{\tau}(\ell, f)$.

The diffusion coefficients, denoted here by D_{obs} , were determined in the long-time regime $\langle [\Delta x(t)]^2 \rangle > \bar{\ell}^2$, as a slope of the mean square displacement via [22]

$$\langle [\Delta x(t)]^2 \rangle \sim 2D_{\text{obs}}t, \quad (8)$$

where $\Delta x(t) = x_p(t_0 + t) - x_p(t_0)$ is the particle displacement during a time interval of length t . In the simulations, to reach the hydrodynamic regime not only for interfaces but for diffusion as well, we run the dynamics long enough so that the square root of $\langle [\Delta x(t)]^2 \rangle$ is much larger than the bubble size. Particle diffusion in the y direction, on the other hand, is in the long-time limit simply controlled by interface wandering and the effective size-dependent diffusion coefficient related to that.

D. Overview of the parameters and their meaning

Our full model for diffusion restricted by fluctuating interfaces contains thus the following variable parameters:

(i) The driving parameter f , defined in Eq. (3) of Sec. II A, drives the interfaces towards each other. For interfaces to be coupled in the steady state we must have $f > 0$. For increasing f , the channel for diffusion becomes narrower and the lengths of the locally open paths, i.e. the bubble sizes, get smaller and the time scale of fluctuations gets longer. For $f \leq 0$ the interfaces would be driven apart of each other and diffusion between them would become an unrestricted random walk.

(ii) The second parameter is the generic jump attempt frequency μ of the diffusing particle. The possible jump directions (horizontal, vertical or diagonal, see also Fig. 1) are controlled by the parameter $m = 1, 2, 3, 4$ described in Sec. II B. The simplest choice is the one-dimensional jumps in the model with $m = 4$, which is a good starting point for analytical arguments for the scaling of diffusion with the model parameters.

(iii) The particle jumps are restricted by the dynamic environment provided by the interfaces. The technical details of this are given in Sec. II B, but there are no additional parameters involved. However, there remains two physically reasonable ways to realize the occasions, when the interfaces would possibly move the particle. This is described in Sec. III B: In scheme (A) the particle is considered in such cases to move together with an interface with its diffusive 'clock' left intact and in (B) its 'clock' is updated after the interface move. The physical meaning of these choices is considered in Sec. VI.

IV. RESULTS FOR INTERFACE DYNAMICS

In this Section we first complement the study of Ref. [18] to characterize the time evolution of the coupled interfaces themselves (without a diffusing particle) in the stationary state. In the observed dynamics, a few time scales of interest can be monitored to gain insight also into the behavior of diffusion between the interfaces to be discussed in the next Section. The first time scale is the average time T_{int} elapsed between consecutive changes in the interface configuration. The second one, denoted by T_{lat} , is the average time scale over which a single location in x direction stays within a bubble $\ell > 0$ in the x direction. Also the third one describes the behavior of the interface system only: It is the average waiting time $T_{\text{bub}}^{(j)}$ for a change in the bubble size,

$$T_{\text{bub}}^{(j)}(f) = \sum_{\ell=j}^{L-1} P_j(\ell, f) \bar{\tau}(\ell, f), \quad (9)$$

where $P_j(\ell, f)$ is the normalized bubble size distribution and $\bar{\tau}(\ell, f)$ is the corresponding average waiting time for something to happen for a bubble of size ℓ , see Sec. III C.

To obtain more detailed information, we computed $T_{\text{bub}}^{(j)}$ for $j = 0, 1, 2$ because the bubbles of size $\ell = 0, 1, 2$ control diffusion for large f .

In Fig. 2 we present the timescales T_{int} , T_{lat} , $T_{\text{bub}}^{(j)}$ describing the interface dynamics. The time T_{int} is determined by the interface configuration and its behavior is not monotonic as can be seen from Fig. 3, where a shallow minimum is observed. On the other hand, the roughness W as a function of f , shown in the same figure, displays a dip at $f_w \approx 0.15$. The non-monotonic behavior is explained by the entropic effects through the reduced configuration space available for the interfaces [18]. The finite-size scaling of the dip position, $f_w(L)$, was studied in Ref. [18], we only mention here the result $f_w \sim L^{-1/3}$ for large L . In passing we note that such a deroughening due to interactions between interfaces has been experimentally observed in another context, see the articles in Ref. [19]. It is evident from Fig. 2 that the point $f = f_w$ is also the crossing point for the dynamical properties of the interfaces. For $f > f_w$, T_{int} increases rapidly and displays the asymptotic behavior $T_{\text{int}} \sim f$ for large f , because the rate-limiting factor is the time required to create new bubbles, which is proportional to $1/q_2 \sim (1 - q_2)/q_2 - 1 \equiv f$ for $q_2 \ll 0$ in this limit.

In Fig. 2 we also observe that $T_{\text{lat}} \sim 1/f$ for $f \ll f_w$. This is controlled by the timescale of (finite) interfaces wandering apart from each other and then back together (effectively biased diffusion), which is proportional to $1/(p_2 - q_2) = 1/(2p_2 - 1) \sim 1/f$. For large f we have $T_{\text{lat}} \rightarrow 1/2$, because the smallest bubbles $\ell = 1$ in this limit disappear with the rate $2q_1 \rightarrow 2$. For increasing f , the time scale $T_{\text{bub}}^{(0)}$ increases without limit with the waiting time for a bubble to appear as $T_{\text{bub}}^{(0)} \sim f$, but $T_{\text{bub}}^{(1)} \rightarrow 1/2$ by the same argument as for T_{lat} . Also the

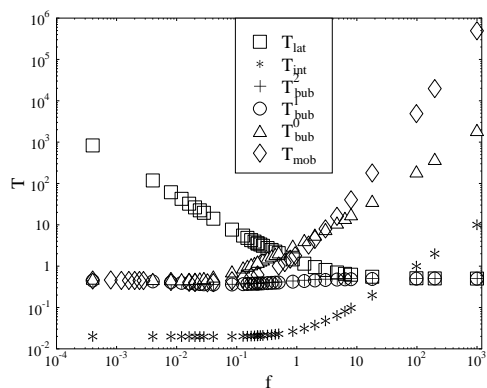


FIG. 2: Characteristic timescales of the interfaces: the site-open time scale T_{lat} , the interface-change time scale T_{int} , the bubble waiting times $T_{\text{bub}}^{(j)}$ for $j = 0, 1, 2$ and the effective mobility time scale T_{mob} .

behavior of $T_{\text{bub}}^{(2)}$ has the same asymptotics, as can easily be seen by inspecting the one and only possible shape of bubbles of size $\ell = 2$, the rate-limiting factor being the shrinking of the bubble from its either end.

The last time scale shown in Fig. 2 is the average waiting time for a change involving a bubble of size $\ell \geq 2$ to occur in a given lattice site, which we denote by T_{mob} , since it is related to configuration changes that change the effective mobility of a particle by increasing or decreasing its possible range of motion. This differs from $T_{\text{bub}}^{(2)}$ in that, for example, for a particle sitting at site x , where the sites belongs to a bubble with $\ell \leq 1$, *i.e.* for a particle stuck in a locally closed configuration, in averaging T_{mob} we count the time for the particle to be mobile again, *i.e.* for the site to be in a bubble with $\ell \geq 2$ again. For a bubble with $\ell > 2$, on the other hand, each change of its size will result in a greater or smaller effective mobility for the diffusing particle. For $f \gg f_w$ we have $T_{\text{mob}} \sim f^2$, since the rate-limiting process contributing to it in this limit is a two-step process, where a bubble of size two becomes created starting from a configuration where there are no bubbles.

To characterize the properties of the interface configurations in more detail, we present in Fig. 4 the mean bubble size $\bar{\ell}$ and the kink density \bar{k} . The non-monotonicity of the differently normalized (see the caption) mean bubble size $\bar{\ell}^*$ is a consequence of the fact that for finite L the maximum size of a bubble is limited. Below the roughness dip, for $f < f_w$, the probability of completely open bubbles ($\ell \geq L$), neglected in the computation of $\bar{\ell}$, rapidly increases for decreasing f , while the number of such bubbles is essentially zero for $f > f_w$. In the vicinity of the dip, for $f \approx f_w$, we observe $\bar{\ell} \sim f^{-4/3}$, but for large f it tends to $\bar{\ell} \sim f^{-1}$, as expected. The kink density has a clear minimum slightly above f_w , which is consistent with the reduction of configuration space

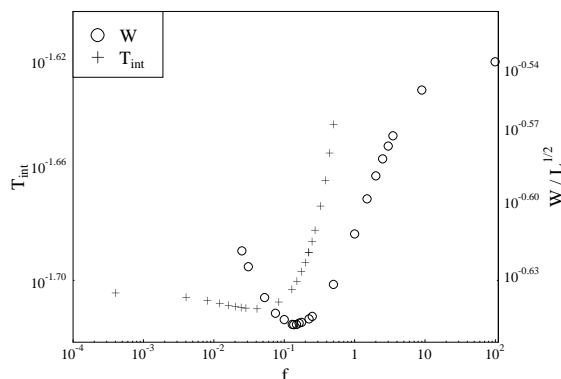


FIG. 3: The T_{int} and the scaled interfacial roughness W . Note that the vertical scale is different for these quantities. For this system size, the roughness dip is observed at $f = f_w \approx 0.15$.

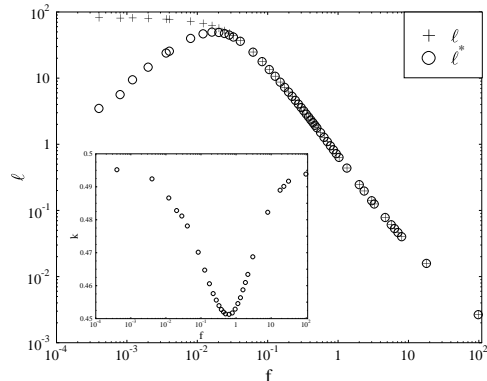


FIG. 4: The average bubble size $\bar{\ell}$ and kink density \bar{k} as a function of f . We show the bubble size normalized in two ways: the real $\bar{\ell}$ where bubble sizes $0 \leq \ell < L$ and $\bar{\ell}^*$ where $0 \leq \ell \leq L$ are taken into account.

due to the interaction between the interfaces, resulting in more hill tops and valley bottoms, which are not kink sites. Note also that $\bar{k}(f \rightarrow 0) = \bar{k}(f \rightarrow \infty)$, because in the latter limit the interfaces are bunched together and their dynamics then reduces to that of a single isolated interface [18].

V. RESULTS FOR PARTICLE DIFFUSION

For a continuous-time unbiased random walk the one-dimensional mean square displacement is of the form [22]

$$\langle [\Delta x(t)]^2 \rangle = \langle N_s \rangle(t) \sigma_{\Delta x}^2, \quad (10)$$

where $\langle N_s \rangle(t)$ denotes the average number of jumps in time t , and $\sigma_{\Delta x}^2$ is the variance of the displacement of individual jumps. In what follows we shall use Eq. (10) to justify a theoretical model for diffusion between the interfaces for $f > f_w$. For the different models of particle dynamics in the presence of the interfaces, *i.e.* the models $m = 1, \dots, 4$ defined in Sec. II B, we shall report our results as a function of the drive parameter f and the total jump rate μ as the dimensionless ratios

$$D_m(f, \mu) = \frac{D_{\text{obs}}^{(m)}(f, \mu)}{D_{\text{free}}^{(m)}(\mu)}, \quad (11)$$

where $D_{\text{obs}}^{(m)}(f, \mu)$ is the observed diffusion coefficient according to Eq. (8) and $D_{\text{free}}^{(m)}(\mu)$ is that corresponding to the same intrinsic jump rates without the interfaces. These ratios then give the effect of the interfaces on diffusion, while μ is the total attempt rate of jumps for the given model in units of the total attempt rate of local interface configuration changes. For a free random walk

with $\sigma_{\Delta x}^2 = 1$, combining Eqs. (17) and (10) gives the diffusion coefficient for free motion in x direction, for example, as $D_{\text{free}}^{(1)} = \alpha = \mu/4$ and $D_{\text{free}}^{(4)} = \nu = \mu/2$. We shall begin our discussion with the simplified dynamics $m = 4$, because for it the generic features of diffusion between the interfaces become more transparent.

A. Diffusion for the one-dimensional particle dynamics (model 4)

In the case of *slow particles* the interface configuration will change many times between the jump attempts of the particle. In this case, the success ratio of the jump attempts can be evaluated from the bubble size distribution $P_0^*(\ell, f)$ and it is

$$g(f) = \sum_{\ell=2}^{L-1} P_0^*(\ell, f) \frac{\ell-1}{\ell} + P_0^*(L, f), \quad (12)$$

because only within bubbles with $\ell \geq 2$ the particles can move and with probability $(\ell-1)/\ell$ is an attempted jump possible since the particle cannot jump out of the bubble so that 2 of the 2ℓ attempts are blocked by the bubble edges. The mean-field prediction for the diffusion coefficient is then

$$D_{\text{mf}}^{(m)}(f, \mu) = g(f) D_{\text{free}}^{(m)}(\mu). \quad (13)$$

The simulation results for the model $m = 4$ together with this mean-field approximation are presented in Fig. 5. For $\mu \ll 1/T_{\text{int}}$, i.e. for slow diffusion, the curves $D_4(f, \mu)$ follow the mean field prediction of Eq. (13).

In the inset of Fig. 5 we show a data collapse by using for f the scaling factor

$$\sigma(\mu) = \sqrt{1 + c\mu} \quad (14)$$

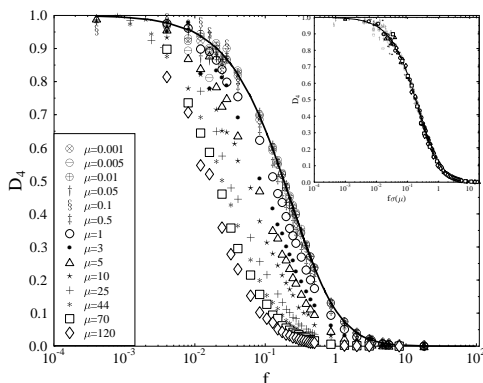


FIG. 5: Simulation results (plotting symbols) for $D_4(\mu, f)$ and the mean-field prediction for the small μ limit (solid line). In the inset we show the data collapse discussed in text.

with $c = 1$. This is an interpolation of the large μ behavior $\sigma(\mu) \sim \mu^{1/2}$ for $\mu \gg 1$, with the interface and particle time scales well separated, and the small μ behavior $\sigma(\mu) \approx 1$ for $\mu \ll 1$, which is exactly the mean-field result discussed above. With this scaling, our simulation data for $D_4(f, \mu)$ for $f < f_w$ is nicely collapsed onto the slow-particle curve defined by Eq. (13) and even better with the choice $c \approx 1.1$ (not shown), which we assign to finite-size effects. However, to obtain a good data collapse for $f > f_w$ we need a different scaling combination,

$$D_{\text{obs}}^{(m)} \rightarrow D_{\text{obs}}^{(m)} / [1 - \exp(-\mu\tau_2)], \quad (15)$$

corresponding to an exponential clock with $\tau_2 = T_{\text{bub}}^{(2)}(f \rightarrow \infty) = 1/2$. This scaling form results from the characteristic time scale of smallest bubbles allowing diffusion of particles in this regime. This is controlled by the driving parameter f such that for $f \gg 1$ there are mainly bubbles of size $\ell = 1$, but for diffusive jumps to take place bubbles of size $\ell = 2$ are needed (with the time units chosen, once created, they stay open at least over one unit of time, cf. Sec. IV). This scaling is demonstrated in the loglog plot of Fig. 6. Because of the different rate-limiting mechanisms these scaling forms, below and above the dip region, are incompatible.

Next we consider the case of *fast particles*. If the particle jump rate is fast compared to the interface dynamics, an adiabatic approximation can be done as follows. The particle is then trapped inside a bubble and its location becomes uniformly distributed in the timescale of the bubble dynamics and the (effective) location of the parti-

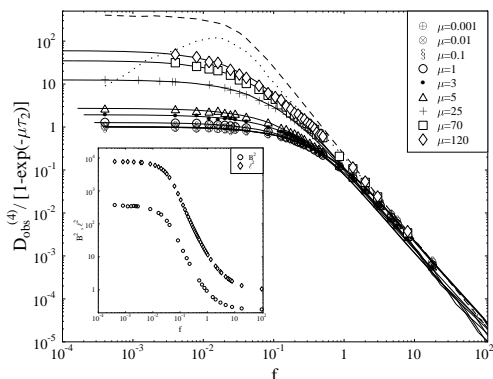


FIG. 6: Data collapse for the large f behavior of $D_{\text{obs}}^{(4)}$ by using the scaling form of Eq. (15). The plotting symbols show the simulation results and the solid lines are the mean-field approximation for small μ of Eq. (13) with f scaled by the factor $\sigma(\mu)$ given in Eq. (14). The dashed line is the adiabatic approximation of Eq. (16) and the dotted line is the finite-size-corrected infinite-rate approximation described in text. In the inset we show the comparison of the behavior of the jump-length factor B^2 and the mean squared bubble size ℓ^2 .

cle can change only when the size of the bubble changes. The length of an effective particle jump via this mechanism is approximately the length of the displacement of the center-of-mass location b of the bubble. By applying Eqs. (8,10) we then obtain

$$D_{\text{adiab}}(\mu, f) = \frac{1}{2} \frac{1}{T_{\text{mob}}} B^2(f), \quad (16)$$

where T_{mob} is the time scale of bubble motion and $B^2(f)$ is the mean-square displacement (per jump) of the bubble obtained from

$$B^q(f) = \langle |b_{\text{new}} - b_{\text{old}}|^q \rangle, \quad (17)$$

with $q = 2$. Here b_{new} and b_{old} are the locations of a bubble before and after the change in the bubble size. This approximation is shown by the dashed line in Fig. 6. For large f the expected behavior $D \sim f^{-2}$ is recovered, since the bubble jump length and thus B^2 becomes a constant for isolated bubbles and $T_{\text{mob}} \sim f^2$. For $f > f_w$, the bubble motion is dominated by increasing or decreasing the bubble size by one lattice unit and, as expected, for fast particles the adiabatic approximation works well. For $f < f_w$, merging and dissociation of bubbles becomes important. We also tested the choice $q = 1$, with the mean jump length squared, giving less weight to long jumps and thus giving a smaller diffusion coefficient for small f (for large f the smallest jumps dominate in any case), but the approximation is not essentially better.

The dotted curve just below the adiabatic approximation shows an approximation obtained by assuming an infinite jump rate of the particle such that after each interface configuration change a new location for the particle is drawn evenly distributed inside a bubble, but such that the particle displacement in the case of a completely open interface configuration is restricted by the system size. A possible way to extend this approximation for smaller f would be to utilize the known form of the bubble-size distribution for large ℓ . This way we obtain a reduction of the diffusion coefficient that seems to work around $f = f_w$ but apparently fails for small f , *c.f.* the behavior of ℓ^* in Fig. 4. Another natural approximation would be to consider the size of the bubble as defining an effective mobility of the diffusing particle. Qualitatively, the behavior of B^2 and the mean squared bubble size ℓ^2 are quite similar, but with incompatible limits for small and large f . Unlike in Eq. (16) for B^2 , it turns out to be difficult to assign a natural rate factor to ℓ^2 to develop a reasonable approximation for the diffusion coefficient.

B. Diffusion for the two-dimensional particle dynamics (models 1,2,3)

We next consider the effect of the 'microscopic' dynamics on diffusion. First, in Fig. 7 we show the diffusion coefficient for dynamics $m = 1$ with the pushes of the particle by the interfaces handled according to clock-updating

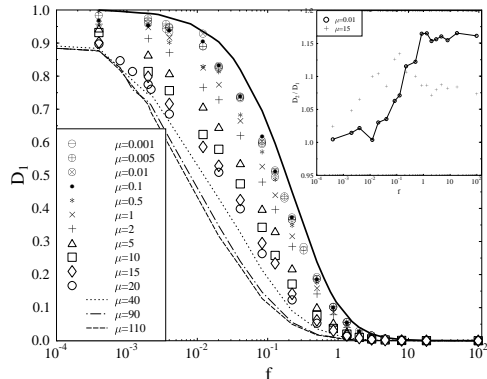


FIG. 7: Diffusion coefficient D_1 for the particle clock updating scheme A. For comparison we show also by the full line the mean-field approximation, *c.f.* Fig. 5. In the inset we show the ratio $D_2(\mu/2)/D_1(\mu)$.

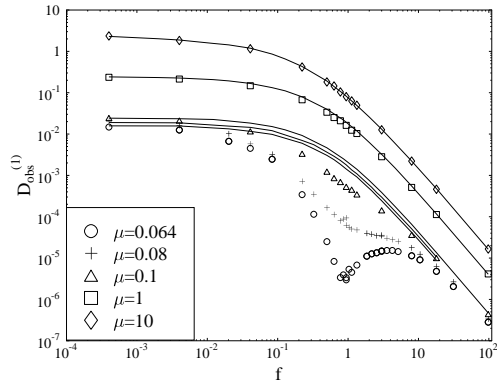


FIG. 8: Diffusion coefficient D_1 for the particle clock updating scheme B. The full curves show the corresponding data for scheme A.

scheme (A) and in Fig. 8 according to scheme (B), see Sec. II B for details. Now it is not just the length of the bubble but also the shape of it that affects diffusion. In (A) the particle waiting time is updated after each jump attempt, in (B) it is updated also after each push by the interfaces. The difference between (A) and (B) appears for long particle waiting times (for small μ) in the regime where there are frequent pushes, *i.e.* the drive f needs to be strong enough, but not so strong that diffusion would be completely dominated by the motion of small bubbles as discussed above. The coincidence of the waiting times of the interface motion and the particle jump attempts produces at a finite value of f in (B) behavior that looks like the suppression of diffusion sometimes observed close

to phase transitions. The dip in D_1 appears close to the dip in the kink density k (see the inset of Fig. 4), where in the local interface configurations there are more sites with possible interface configuration changes (at a kink site the interface is locally frozen) and thus more pushes. Other variants of the jump rate modification are conceivable, *e.g.* physically it might happen that the contact with the interfaces could boost the particle jump rates, but in the region of the parameter space, where bubble dynamics is the rate-limiting factor, it would not essentially change diffusion from what what is observed in scheme (A).

The corresponding mean-field approximation of Eq. (13) shown in Fig. 7 by the full curve is presented to help the comparison between $m = 1$ and $m = 4$. As evident from the comparison of Fig. 7 and Fig. 5, scaling by the factor $\sigma(\mu)$ of Eq. 14 would not yield a very good data collapse for $f \ll f_w$ in the case of two-dimensional particle dynamics. For particles fast both in the horizontal and vertical direction, the blocking of diffusion by 'collisions' with the interfaces is quite efficient and leads to a considerable reduction of D_1 in this regime. Note that even for small f we have $D_1 < 1$ for fast particles, since particle diffusion in the vertical direction is faster than that of the interfaces for any $f > 0$. This in part explains the spreading of the curves $D_1(f)$ for $f < f_w$. In the inset of Fig. 7 we show also the difference between the particle dynamics $m = 1$ and $m = 2$ with the clock updating scheme A (concerning dynamics $m = 3$, we find that $D_1 \leq D_3 \leq D_2$). For reasonable comparison, the jump rates for each dynamics have been chosen such that the total jump rates in the x direction match, thus we plot $D_2(\mu/2)/D_1(\mu)$. Due to the limited accuracy of D_m , the ratio D_2/D_1 becomes somewhat noisy, but a few general observations can be made. A difference first develops for $f > f_w$, because diffusion becomes more restricted by the interfaces within bubbles of the type seen on the right ($x = 17, \dots, 20$) in the snapshot of Fig. 1 becoming prevalent. In such interface configurations, many of the 'horizontal' jumps (for $m = 1$) become blocked and diffusion along the narrow channel requires also 'vertical' jumps, while the diagonal jumps (for $m = 2$) are more effective for particle transport. However, for $f \gg f_w$ diffusion again becomes dominated by bubble motion the way it was for $m = 4$, and $D_m \sim f^{-2}$ for $m = 1, 2, 3$ for both particle clock updating schemes (A) and (B) as seen in Fig. 8.

VI. DISCUSSION

To summarize, we have considered one and two dimensional continuous time random walkers constrained between two evolving interfaces symmetrically driven towards each other. A surprisingly complicated phenomenology appears. First, in the interface model itself there is a dip in the interface roughness at a finite value f_w of the parameter f describing the drive of the inter-

faces against each other [18], with different kinds of interface and bubble dynamics below and above the dip. The crossover from bubble-dominated (interface-dominated) to almost free diffusion is controlled by the relative jump rate of the particle and its interplay with the rate of the interface time evolution. In the analysis of this crossover, simple scaling arguments for the two regimes are incompatible, both physically and formally, so that the full behavior of diffusion cannot be described by a single scaling form. This can be expected to be a generic property of transport restricted by fluctuating interfaces.

Furthermore, diffusion was found to depend on the microscopic details of the interaction between the interfaces and the diffusing particles. In particular, its immediate effect on the waiting time of particle jumps was shown to be considerable, especially for dynamics physically corresponding to diffusion on a lattice in the large-friction limit, which can be realized at domain boundaries in adsorption systems. In a spatial continuum this effect would be absent, as would be the roughness dip. However, the finite-size case, with the underlying microscopic structure not washed out in coarse graining, can be of interest in its own right in nanoscale applications. Then also the size of the channel for the particles will induce a relevant length scale, in addition to the length scale related to the diffusive jumps (lattice) and the one related to the environment (bubbles).

In this work we have considered diffusion that is effectively one-dimensional even if the diffusive jumps and interactions between the tracer particles and the interfaces result from two-dimensional dynamics. The environment for the diffusing particles is then described by a chain of bubbles, where as in higher dimensions more complicated topologies (networks) would arise, in some cases leading to a percolation problem. In such studies, like in the present one, a considerable problem is the wide gap between the 'microscopic' timescales related to the dynamics of the particles and the environment, and the 'hydrodynamic' timescale corresponding to diffusion over length scales larger than any structures in the environment experienced by the particles. We hope our work would inspire further theoretical and experimental studies of diffusion in evolving and constraining environments.

Acknowledgments

We thank Dr. Otto Pulkkinen for useful discussions.

-
- [1] W. Sparreboom, A. van den Berg, and J. C. T. Eijkel, *New J. of Physics* **12**, 015004 (2010); N. F. Y. Durand, C. Dellagiacoma, and R. Goetschmann, A. Bertsch, I. Marki, T. Lasser, P. Renaud, *Ann. Chem.* **12**, 5407 (2009).
- [2] F. Solomon, *Ann. Prob.* **3**, 1 (1975).
- [3] H. Kesten, M. V. Kozlov, and F. Spitzer, *Compositio Math.* **33**, 145 (1975).
- [4] O. Zeitouni, *J. Phys. A: Math. Gen.* **39**, R433 (2006).
- [5] S. Alexander, J. Bernasconi, W. R. Schneider, and R. Orbach, *Reviews of Modern Physics* **53**, 2 (1981).
- [6] P. Le Doussal, C. Monthus, and D. S. Fisher, *Phys. Rev. E* **59**, 4795 (1999).
- [7] Z. Sadjadi and M. F. Miri, *Phys. Rev. E* **78**, 061114 (2008).
- [8] Y. G. Sinai, *Theory of Prob. and Appl.* **27**, 247 (1982).
- [9] K. Boldrighini, R. A. Minlos, and A. Pellegrinotti, *Russian Math. Surveys* **62**, 663 (2007).
- [10] B. Mehlig, M. Wilkinson, V. Bezuglyy, K. Gustavsson, and K. Nakamura, *Phys. Rev. E* **80**, 011139 (2009).
- [11] P. S. Burada, P. Hänggi, and F. Marchesoni, *ChemPhysChem* **10**, 45 (2009).
- [12] M. Evans and T. Hanney, *J. Phys. A: Math. Gen.* **38**, R195 (2005).
- [13] F. Spitzer, *Adv. Math.* **5**, 246 (1970).
- [14] M. R. Evans and T. Hanney, *J. Phys. A: Math. Gen.* **36**, L441 (2003).
- [15] J. Sane, J. Padding, and A. A. Louis, *Faraday Discuss.* **144**, 285 (2010), arXiv:0905.1293.
- [16] C. Kunert and J. Harting, *Phys. Rev. Lett.* **99**, 176001 (2007).
- [17] C. Chevalier and F. Debbasch, *Europhys. Lett.* **89**, 38001 (2010).
- [18] J. Juntunen, O. Pulkkinen, and J. Merikoski, *Phys. Rev. E* **76**, 041607 (2007).
- [19] M. Bauer, A Mougín, J. P. Jamet, V. Repain, J. Ferre, R. L. Stamps, H. Bernas, and C. Chappert, *Phys. Rev. Lett.* **94**, 207211 (2005); P. J. Metaxas, R. L. Stamps, J. P. Jamet, J. Ferre, V. Baltz, B. Rodmacq, and P. Politi, *Phys. Rev. Lett.* **104**, 237206 (2010).
- [20] A.-L. Barabasi and E. H. Stanley, *Fractal Concepts in a Surface Growth* (Cambridge University Press, Cambridge, England, 1995).
- [21] A. B. Bortz, M. H. Kalos, and J. L. Lebowitz, *J. Comp. Phys.* **17**, 10 (1975).
- [22] J. W. Haus and K. W. Kehr, *Phys. Rep.* **150**, 263 (1987).